Молодые галактики на красном смещении больше 9: новые данные и парадигма

Сильченко О.К.
ГАИШ МГУ

Сессия-конференция ОФН РАН,
посвященная 70-летию В.А.Рубакова

Что обещала LCDM-модель по поводу рождения галактик?

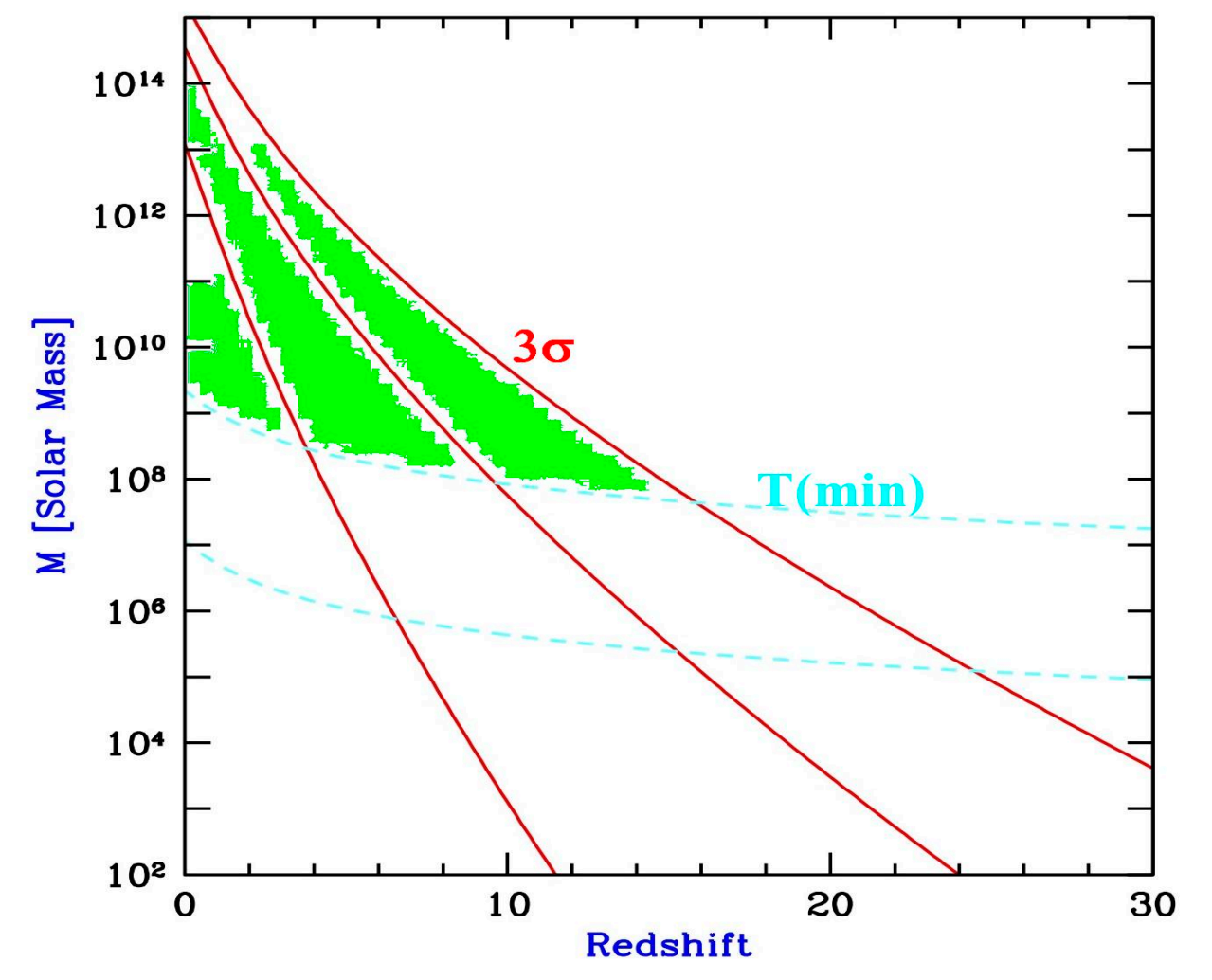

Barkana & Loeb (2001)

JWST-телескоп

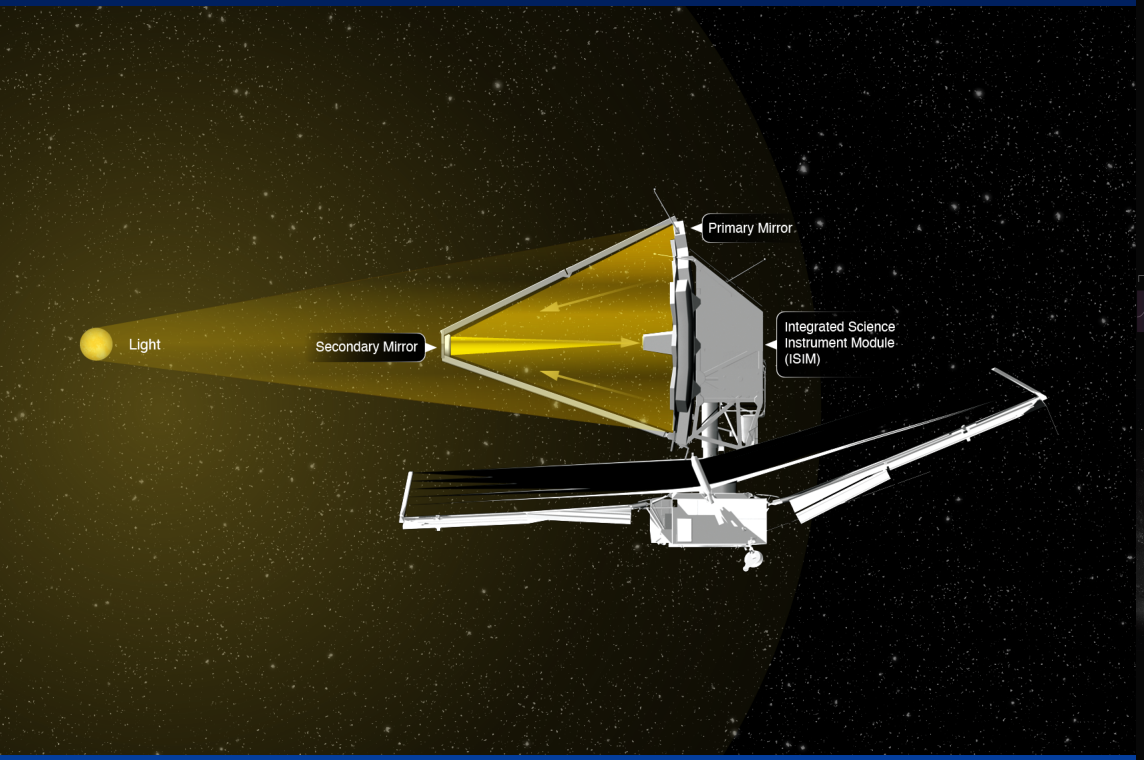

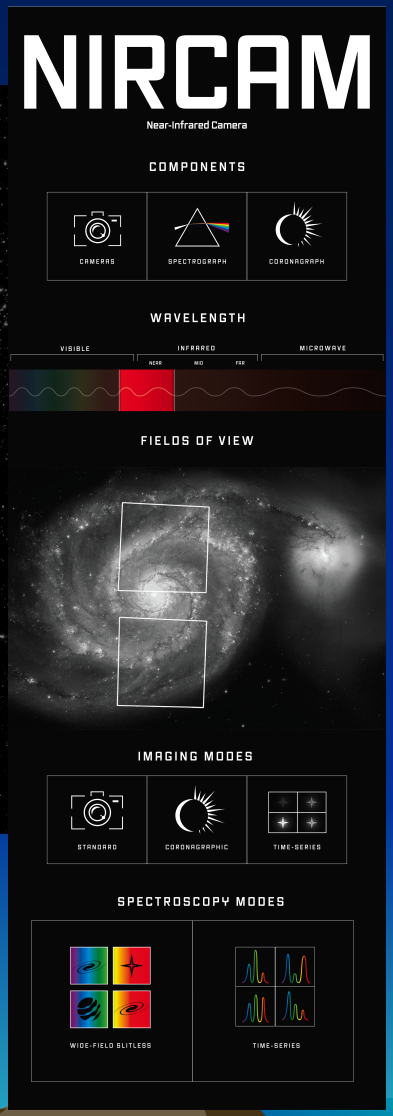

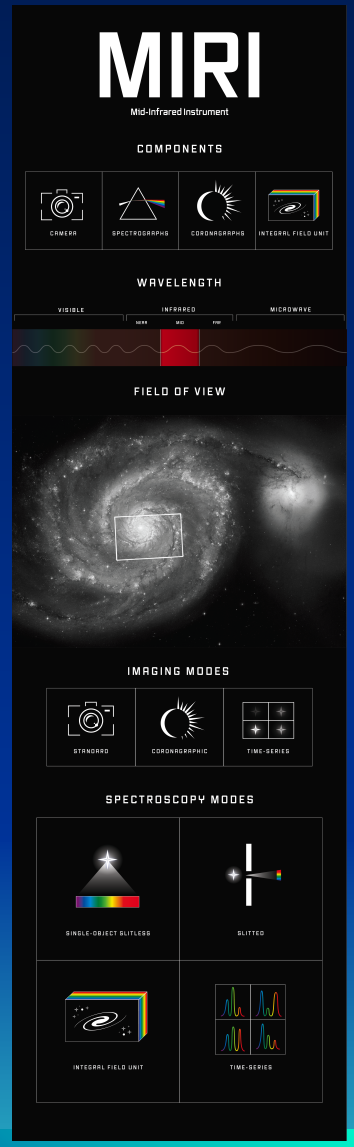

1-4.5 мкм

5-28 мкм

Большое зеркало JWST обеспечивает хорошее пространственное разрешение

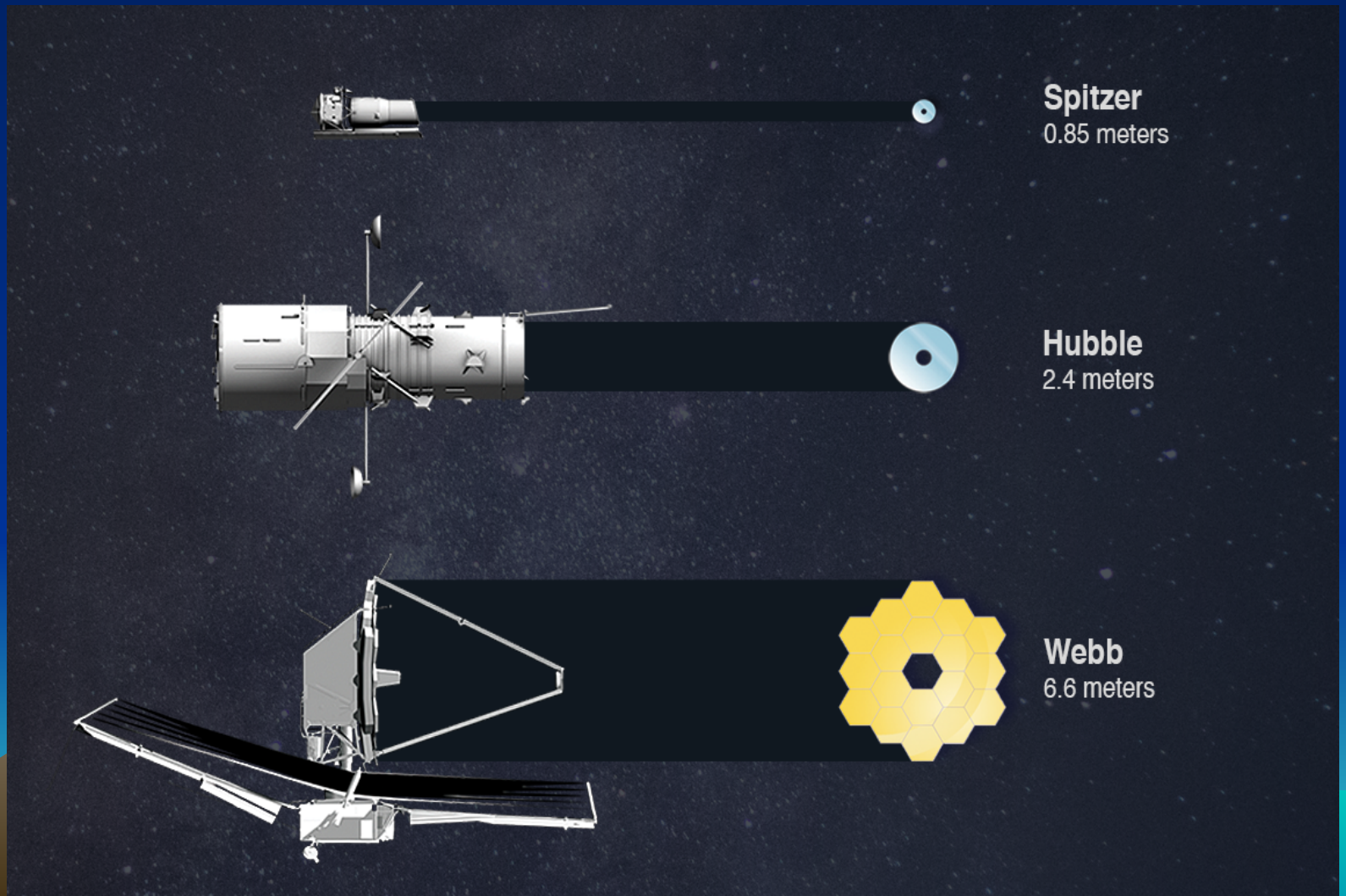

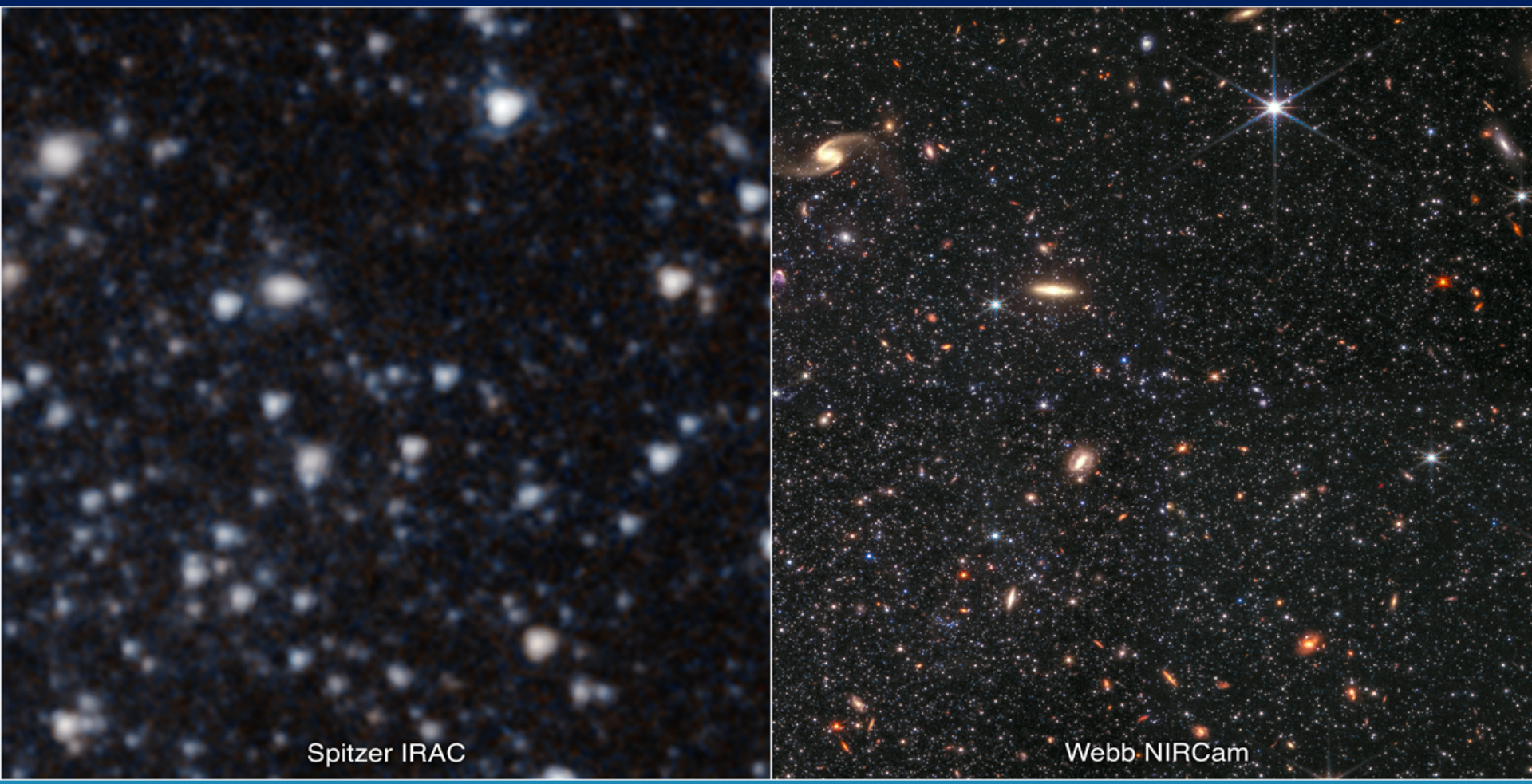
Spitzer IRAC
Webb NIRCam

‘Ly-break’ – самый популярный способ поиска галактик на ранних стадиях эволюции

z=11

z=8

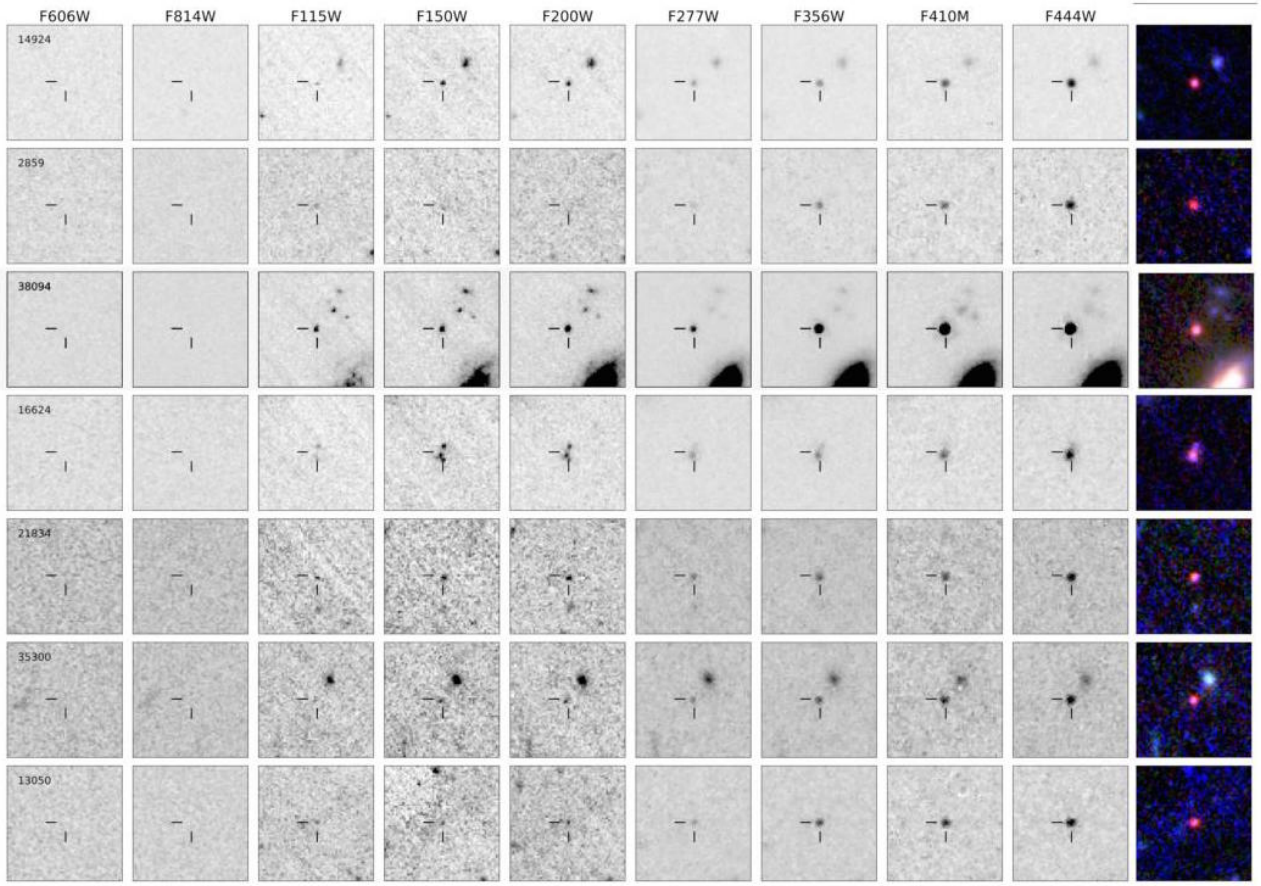

Figure 2: Images of the seven galaxies with $\log(M_*/\mathrm{M}_\odot) > 10.0$ as a function of wavelength. Each cutout has a size of $2.4'' \times 2.4''$. The filters range from the $0.6\,\mu$m F606W filter of *HST*/ACS to the $4.4\,\mu$m F444W *JWST*/NIRCam filter. The galaxies are undetected in the optical filters; blue in the short-wavelength NIRCam filters; and red in the long-wavelength NIRCam filters. Galaxy 38094 has two neighbors at $1''$ distance and the same photometric redshift, indicating an early group or proto-cluster.

JWST расширил спектральный диапазон по сравнению с HST

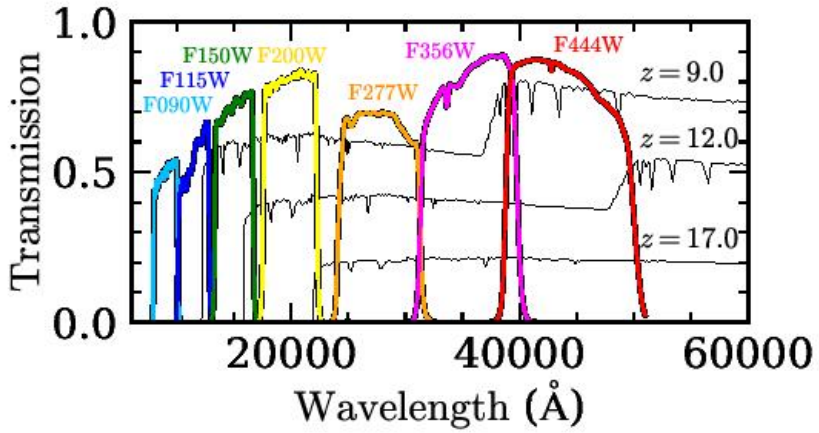

Figure 1. Transmissions of the seven NIRCam broadband filters (cyan: F090W, blue: F115W, green: F150W, yellow: F200W, orange: F277W, magenta: F356W, red: F444W) together with three spectra of star-forming galaxies at z = 9.0, 12.0, and 17.0 from the Bruzual & Charlot (2003) library (black lines).

13 площадок, с данными HST, VLT, Chandra...

Table 4. Limiting Magnitudes and PSF FWHMs of the JWST NIRCam Images for Size Analysis

	5σ Depth / 10σ Depth / PSF FWHM			
Field	F150W	F200W	F277W	F444W
GLASS	29.4 / 28.6 / 0.″0704	29.5 / 28.7 / 0.″0776	—	29.6 / 28.8 / 0.″1605
CEERS	—	29.7 / 28.9 / 0.″0795	29.5 / 28.7 / 0.″1218	—
SMACS J0723	—	29.8 / 29.0 / 0.″0765	—	—
Stephan's Quintet	—	28.0 / 27.2 / 0.″0771	28.7 / 27.9 / 0.″1197	—

NOTE— Limiting magnitudes are measured with randomly distributed 0.″2 diameter circular apertures (Harikane et al. 2022).

Но без спектрального подтверждения красного смещения
это только КАНДИДАТЫ в далекие

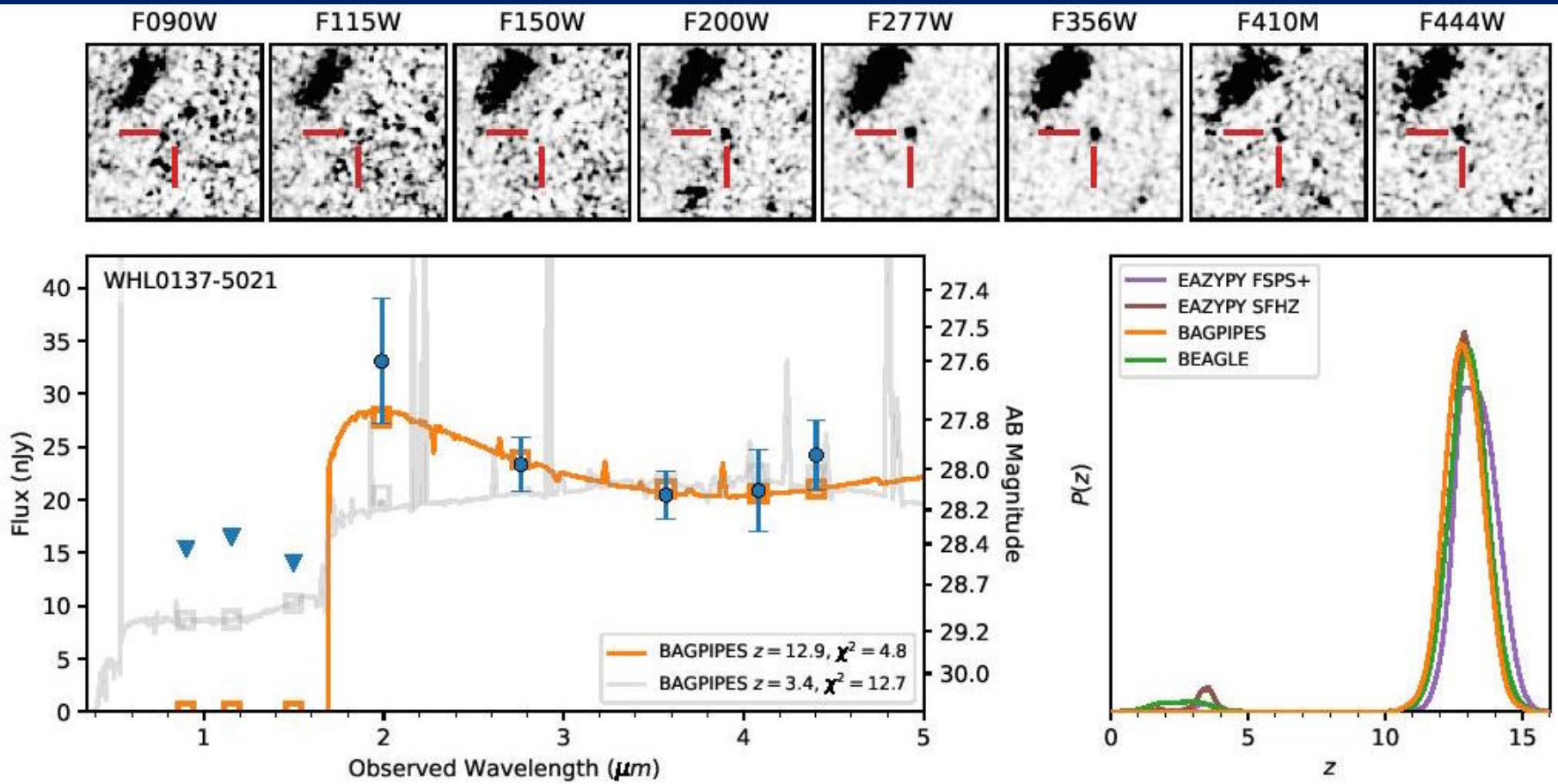

Bradley+(2022)

Спектры: линии и ‘break’

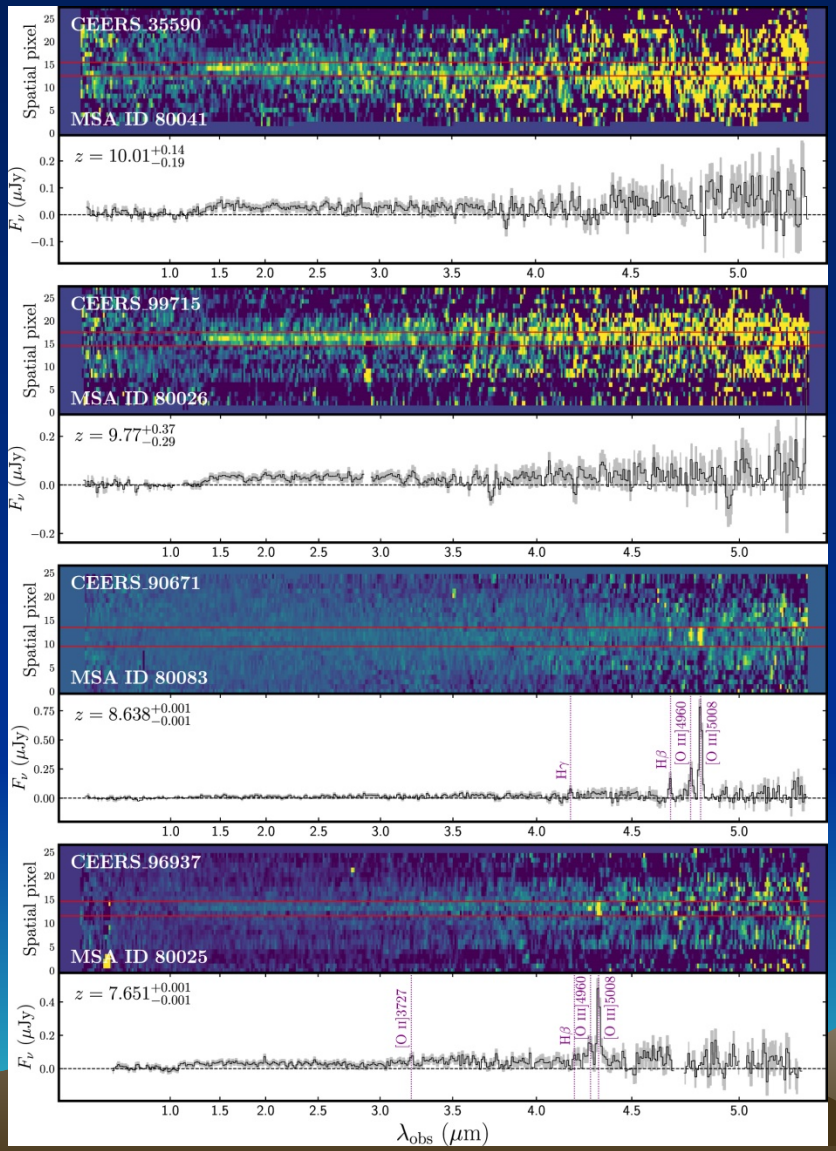

- Спектры JWST/NIR: линии видны, только если z<9
- Когда линий нет – приходится ориентироваться на брейки; но они могут быть как лаймановскими, так и бальмеровскими

Arrabal+2023

Но кое-что получается и на z=11

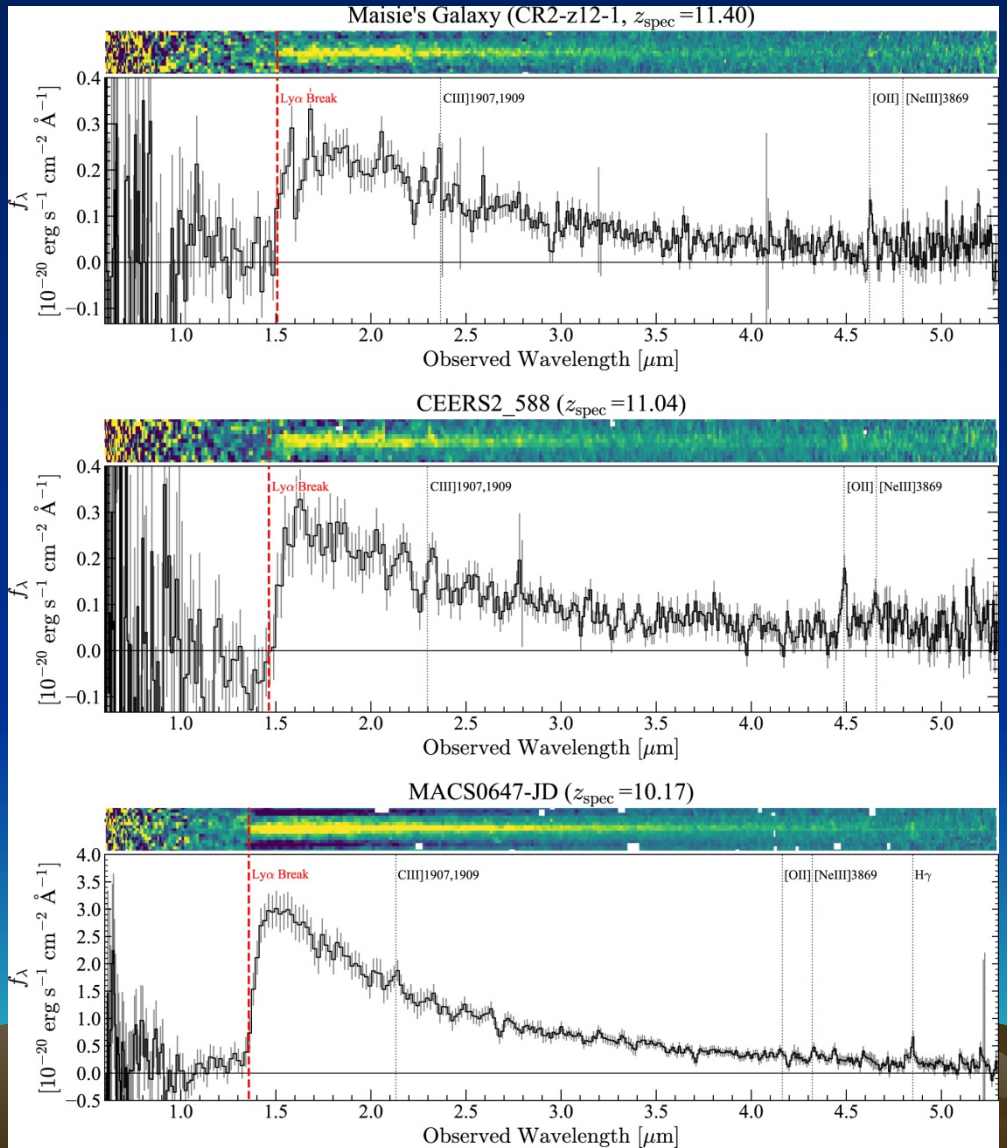

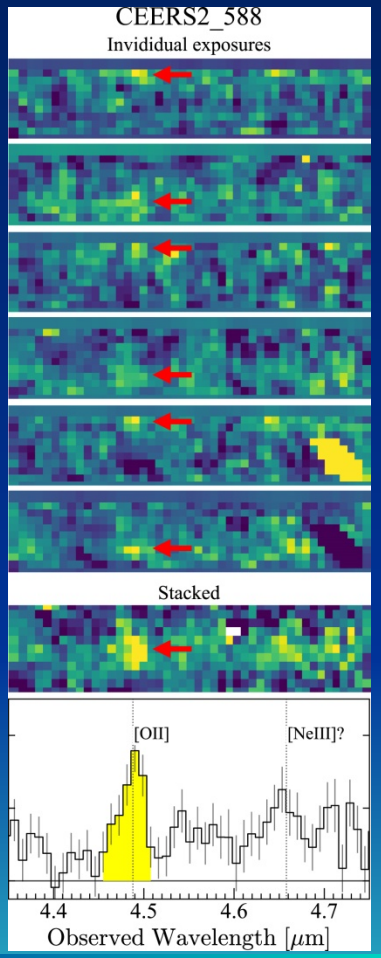

Harikane+(2024)

…и даже на z=12.3! Если привлечь MIRI…

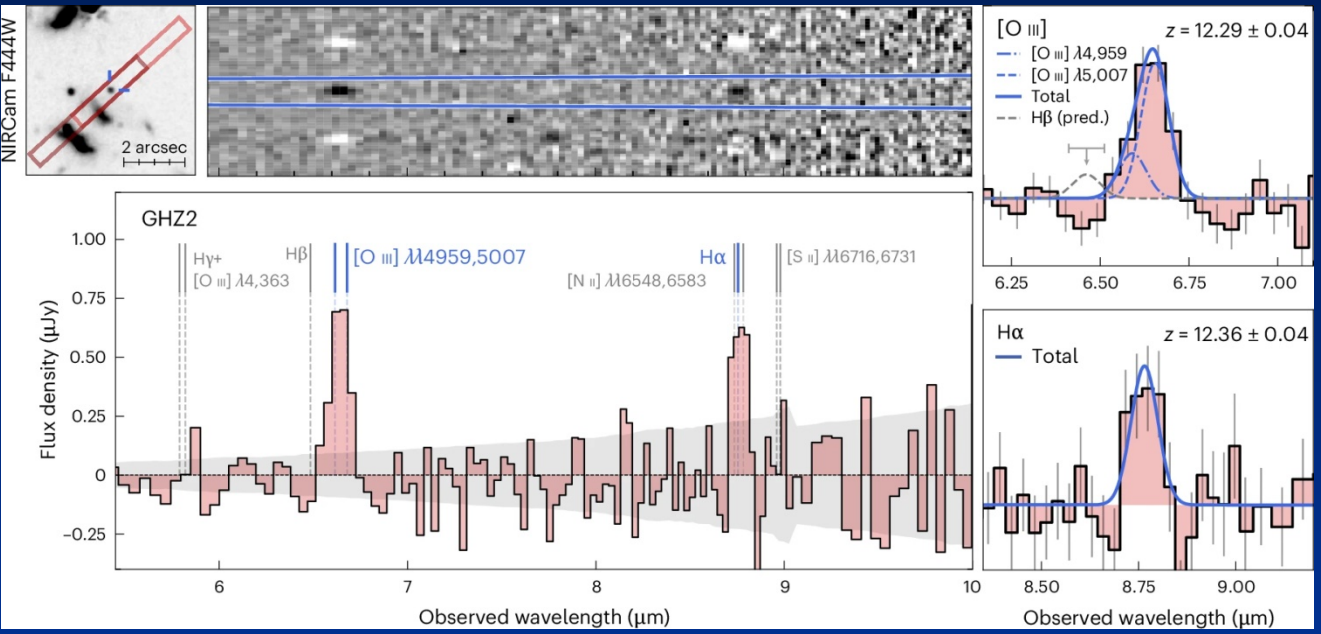

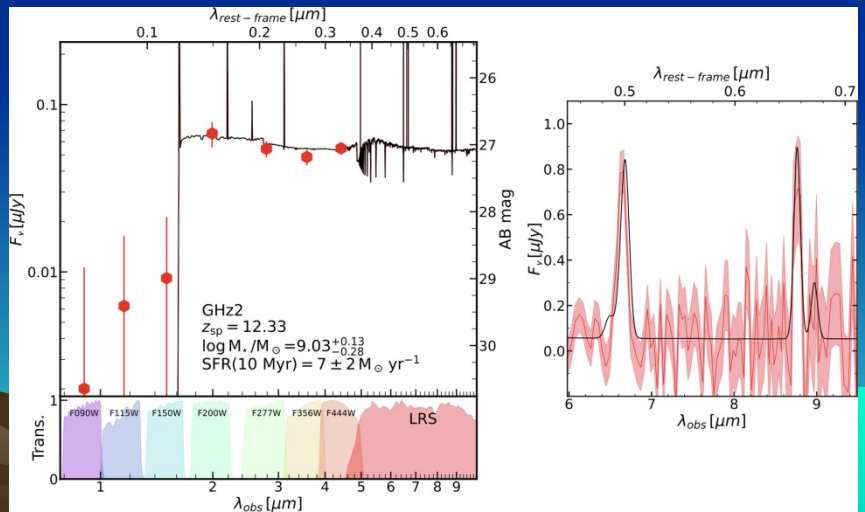

Миллиметровый интерферометр ALMA – такое же разрешение!

ЗАКРЫЛИ z>16!

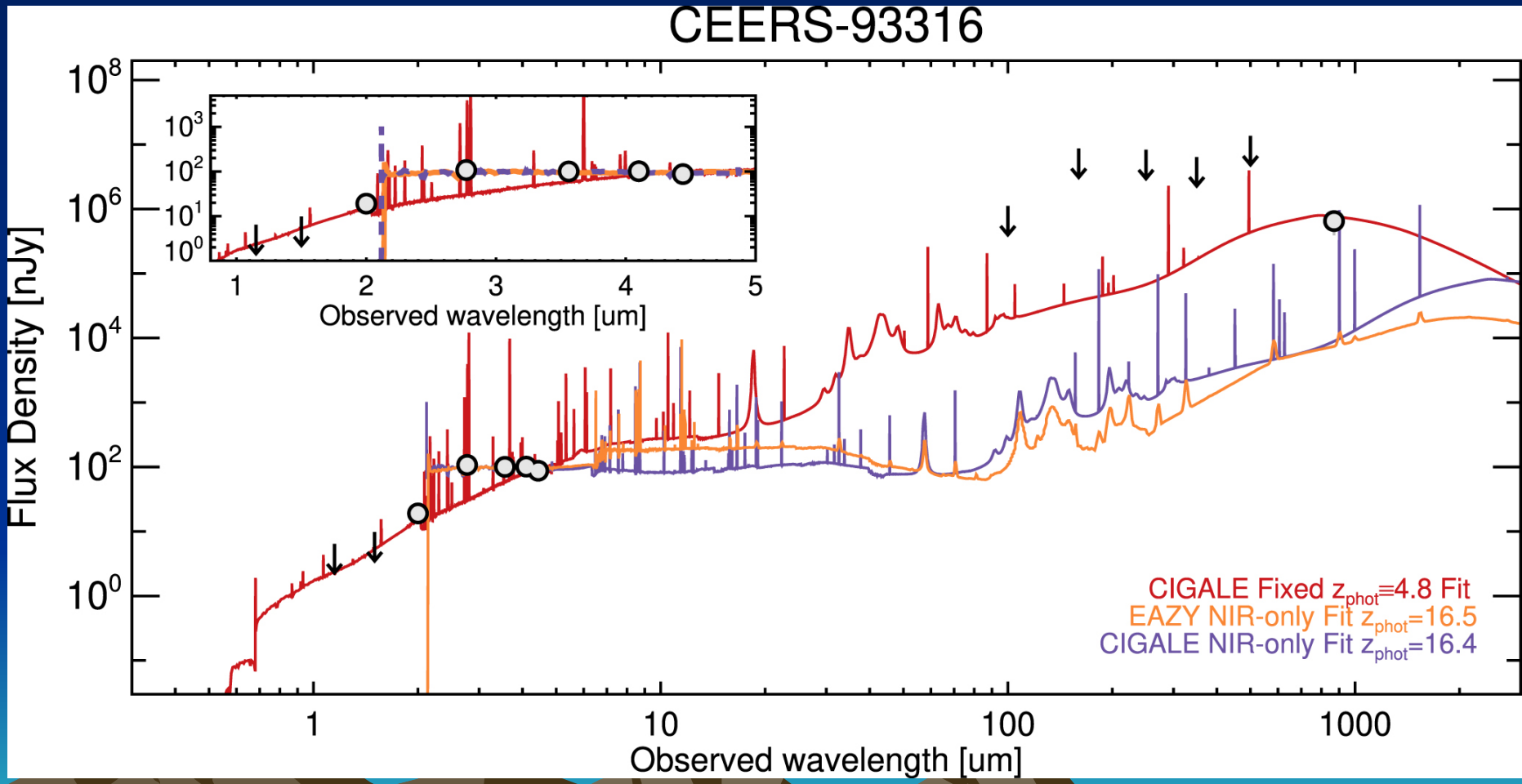

Zavala+ 2023

Но зато подтвердили z=14.2 с эмиссией [OIII]88мкм!

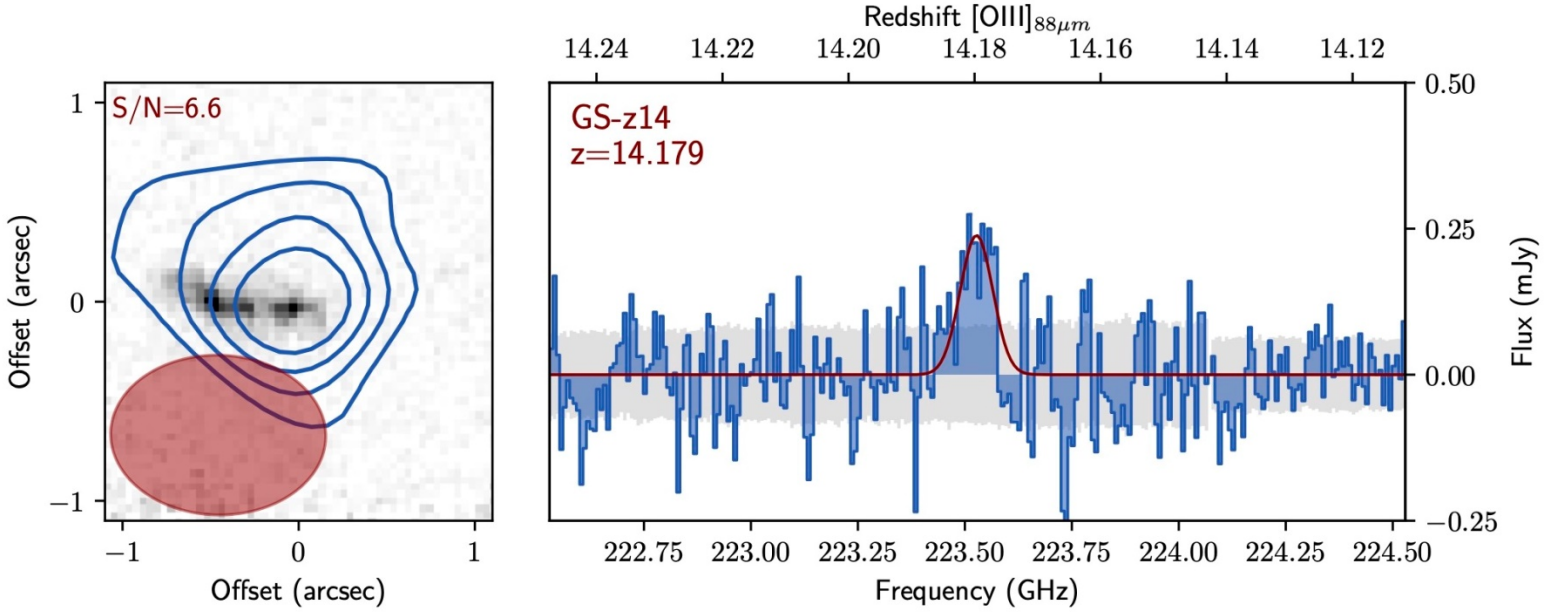

Figure 2. Detection of [OIII]$_{88\mu m}$ in GS-z14 at $z = 14.1793 \pm 0.0007$. *Left Panel:* Contours showing the [OIII]$_{88\mu m}$ emission (2, 3, 4 and 5σ) overlaid on the F200W imaging (Eisenstein et al. 2023a,b). The [OIII]$_{88\mu m}$ emission is detected at a peak significance of 6.6σ in the collapsed data-cube. *Right Panel:* The spectrum of the [OIII]$_{88\mu m}$ line (*blue histogram*) extracted from the >3σ emission region in the moment-0 map. The red line shows the Gaussian fit used to measure the spectroscopic redshift and FWHM of the line. The grey shaded region indicates the 1σ uncertainties.

Вот такие любопытные свойства у этой галактики…

Table 2: Summary of the parameters, prior probabilities and posterior probabilities of the fiducial `prospector` SED model (see also Fig. 5a).

	Parameter (1)	Free (2)	Description (3)	Prior (4)	Posterior (5)
Star-forming component	$z_{\rm obs}$	Y	redshift	$\mathcal{N}(z_{\rm spec}, 0.001)$	$14.178^{+0.001}_{-0.001}$
	$\log M_\star[{\rm M}_\odot\,\mu^{-1}]^\dagger$	Y	total stellar mass formed	$\mathcal{U}(6, 10)$	$8.84^{+0.09}_{-0.10}$
	$\log Z[{\rm Z}_\odot]$	Y	stellar and gas metallicity	$\mathcal{U}(-2, 0)$	$-0.75^{+0.03}_{-0.03}$
	log SFR ratios	Y	ratio of the log SFR of non-parametric SFH	$\mathcal{T}(R(z)^\ddagger, 1, 2)$	—
	$\sigma_\star$ [km s^{-1}]	Y	stellar intrinsic velocity dispersion	$\mathcal{U}(0, 300)$	190^{+70}_{-70}
	n	Y	power-law modifier of the dust curve (T22, their eq. 5)	$\mathcal{G}(0, 0.1; -1.0, 0.2)$	$0.06^{+0.05}_{-0.04}$
	τ_V	Y	optical depth of the diffuse dust (T22, their eq. 5)	$\mathcal{U}(0, 2)$	$0.12^{+0.03}_{-0.03}$
	$\mu_{\rm d}$	Y	ratio of optical depths of the birth clouds and τ_V	$\mathcal{G}(1, 0.1; 0, 2)$	$0.94^{+0.06}_{-0.07}$
	$\sigma_{\rm gas}$ [km s^{-1}]	Y	intrinsic velocity dispersion of the star-forming gas	$\mathcal{U}(0, 1500)$	$1,310^{+90}_{-100}$
	$\log U$	Y	ionization parameter of the star-forming gas	$\mathcal{U}(-4, -1)$	$-2.39^{+0.23}_{-0.19}$
	$f_{\rm esc}$	Y	birth-cloud escape fraction of ionizing radiation	$\mathcal{U}(0, 1)$	$0.18^{+0.10}_{-0.09}$
	$\log N_{\rm H\,I}$	Y	column density of neutral hydrogen	$\mathcal{U}(17, 25)$	$21.97^{+0.07}_{-0.08}$
Other	$j_{\rm spec}$	Y	multiplicative noise inflation term for spectrum	$\mathcal{U}(0.5, 2)$	$1.5^{+0.3}_{-0.4}$
	$\log SFR_{10}[{\rm M}_\odot\,{\rm yr}^{-1}\,\mu^{-1}]^\dagger$	N	star-formation rate averaged over the last 10 Myr	—	$1.00^{+0.08}_{-0.09}$
	$\log SFR_{100}[{\rm M}_\odot\,{\rm yr}^{-1}\,\mu^{-1}]^\dagger$	N	star-formation rate averaged over the last 100 Myr	—	$0.75^{+0.10}_{-0.11}$
	$F_{[{\rm O\,III}]}[10^{-19}\,{\rm erg\,s^{-1}\,cm^{-2}}]$	N	FIR [O III] line flux	—	$3.48^{+1.09}_{-0.85}$
	[O III]λ5007/Hβ	N	Emission-line ratio	—	$4.2^{+0.5}_{-0.6}$
	age [Myr]	N	Mass-weighted stellar age	—	40 ± 5

(1) Parameter name and units (where applicable). (2) Only parameters marked with 'Y' are optimized by `prospector`; parameters marked with 'N' are either tied to other parameters (see Column 4), or are calculated after the fit from the posterior distribution (in this case, Column 4 is empty). (3) Parameter description. (4) Parameter prior probability distribution; $\mathcal{N}(\mu, \sigma)$ is the normal distribution with mean μ and dispersion σ; $\mathcal{U}(a, b)$ is the uniform distribution between a and b; $\mathcal{T}(\mu, \sigma, \nu)$ is the Student's t distribution with mean μ, dispersion σ and ν degrees of freedom; $\mathcal{G}(\mu, \sigma; a, b)$ is the normal distribution with mean μ and dispersion σ, truncated between a and b. (5) Median and 16$^{\rm th}$–84$^{\rm th}$ percentile range of the marginalised posterior distribution; for some nuisance parameters we do not present the posterior statistics (e.g., log SFR ratios). † We corrected all extensive quantities for gravitational lensing, using $\mu = 1.17$ (Carniani et al. 2024). ‡ The non-parametric SFH is expressed by the logarithm of the SFR between adjacent time bins; we use a 'rising' SFH probability prior, which at each time bin is a $\mathcal{T}$ distribution with mean log ratio $R(z) \equiv \log\,(SFR(z_i)/SFR(z_{i+1}))$, where z_i is the redshift of the $i^{\rm th}$ SFH bin and the $SFR(z)$ is given by Turner C. et al. (in prep.), their eq. (4).

Полная выборка CEERS: ‘ранний релиз’

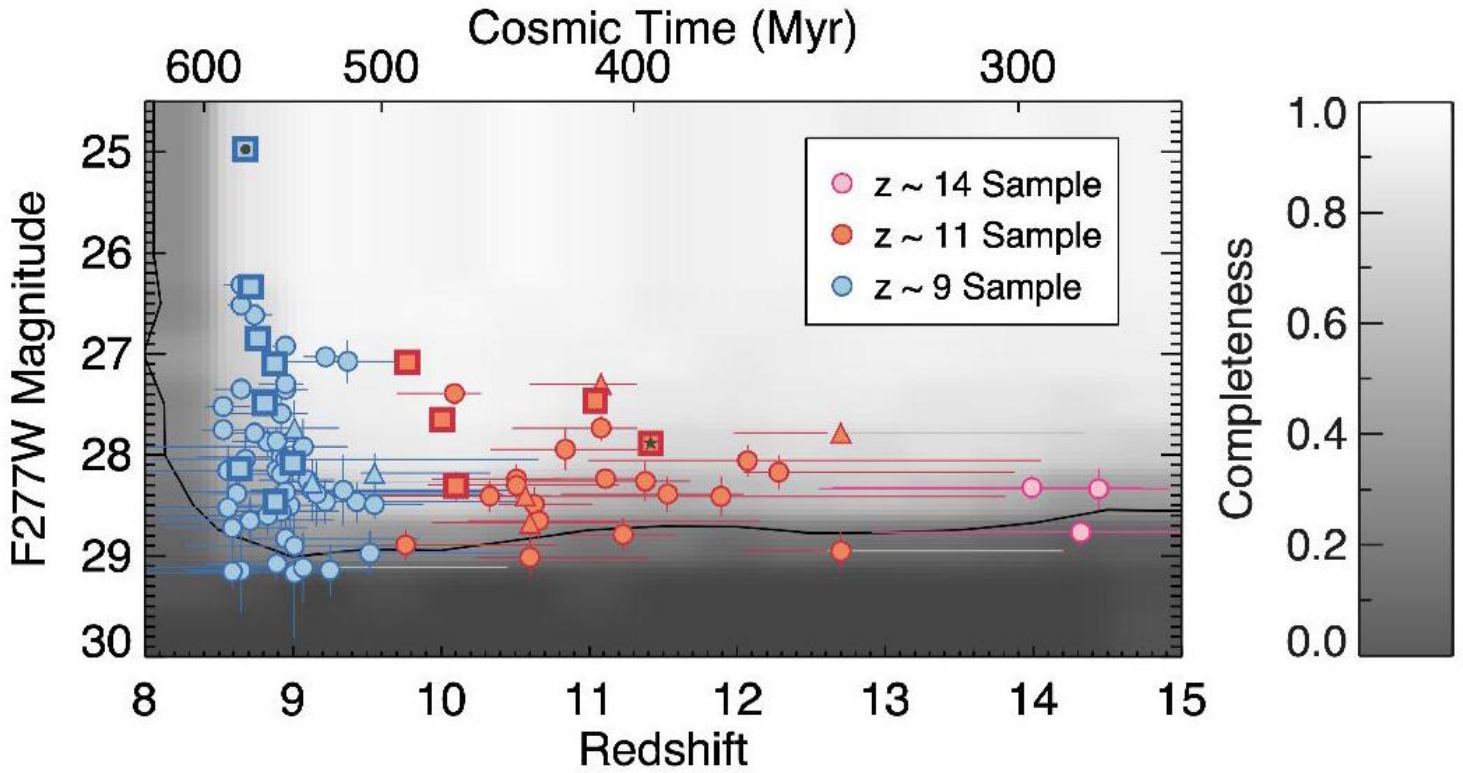

Figure 3. The symbols show our sample of 88 $z > 8.5$ galaxy candidates in a plane of F277W magnitude versus redshift, with the different colors representing the different redshift samples. Squares denote objects with spectroscopic confirmation, while the circles are plotted at the photometric redshifts. Triangles denote objects with spectroscopic observations but no confirmation. The small star denotes Maisie's Galaxy (Finkelstein et al. 2022b), one of the first *JWST* very high-redshift galaxy discoveries, while the small dot denotes CEERS-1019, a confirmed $z = 8.7$ galaxy which appears to have broad Hβ emission, indicative of an active super-massive black hole (Larson et al. 2023). The background shading shows the completeness (inclusive of both photometric and sample selection completeness) of our sample (for sources with half-light radii of 3.3 pixels), as described in §4.1; the black line shows the 20% completeness contour.

Finkelstein+(2023): 88 галактик

Слишком много ярких галактик на z>10

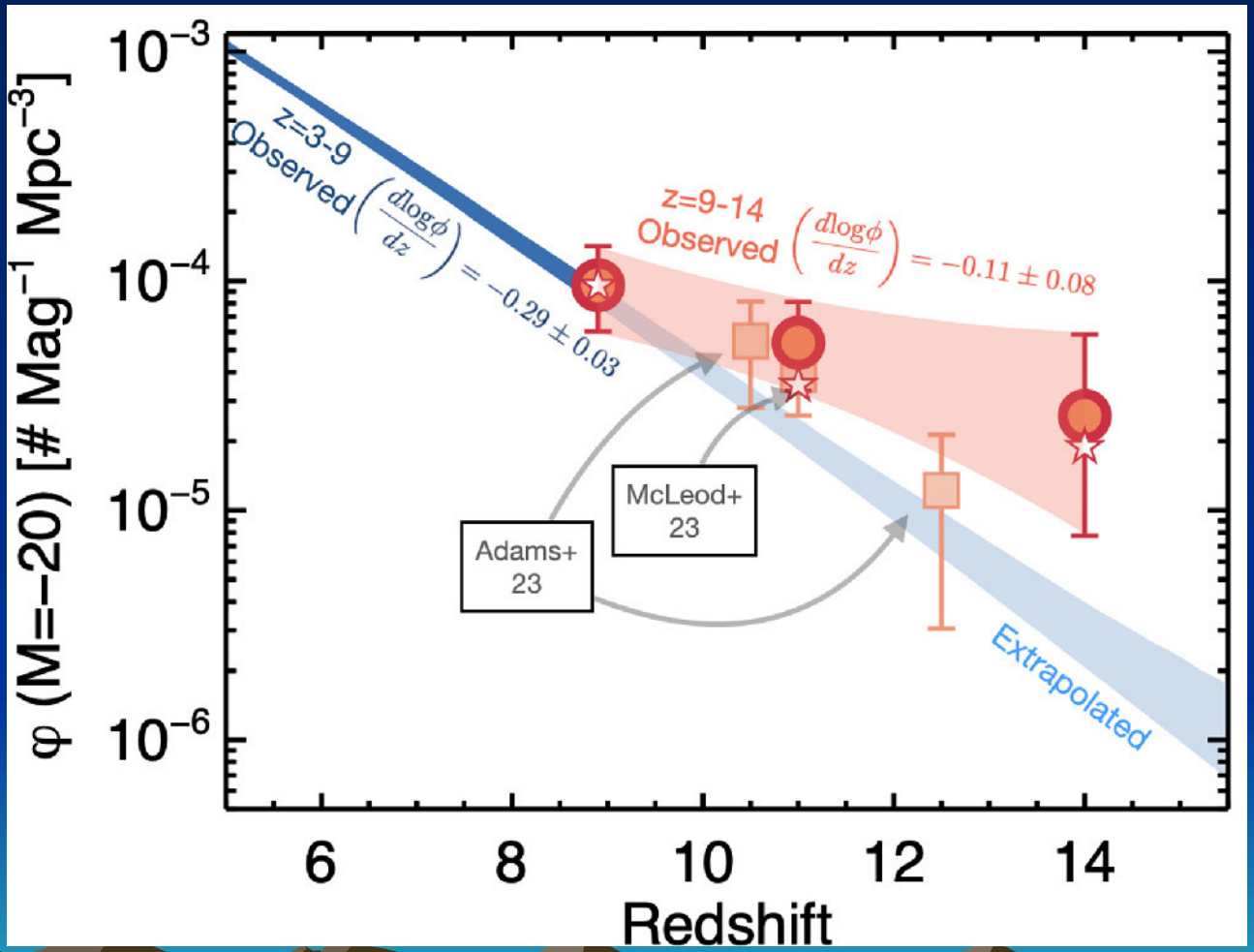

Finkelstein+2024

Причем ярких именно в УФ…

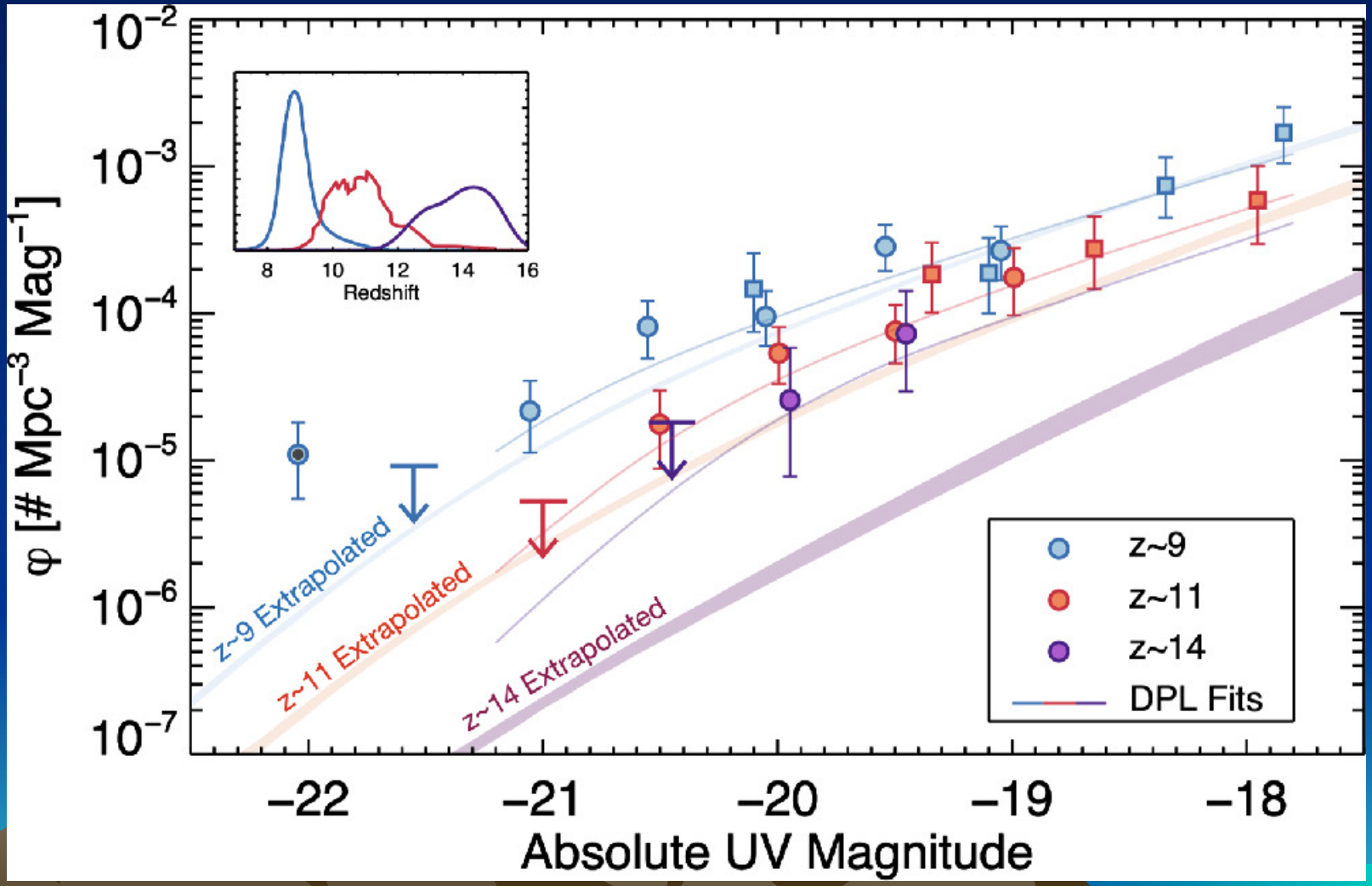

Finkelstein+(2024)

Повышенная эффективность звездообразования?

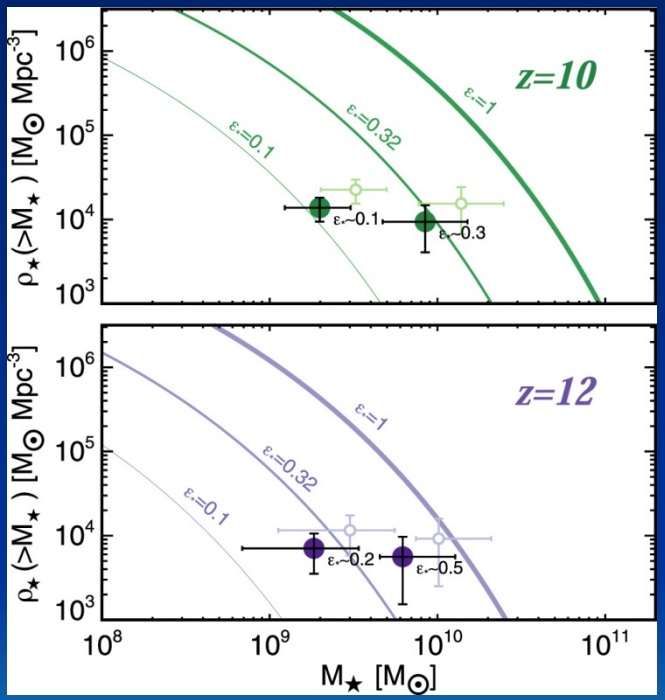

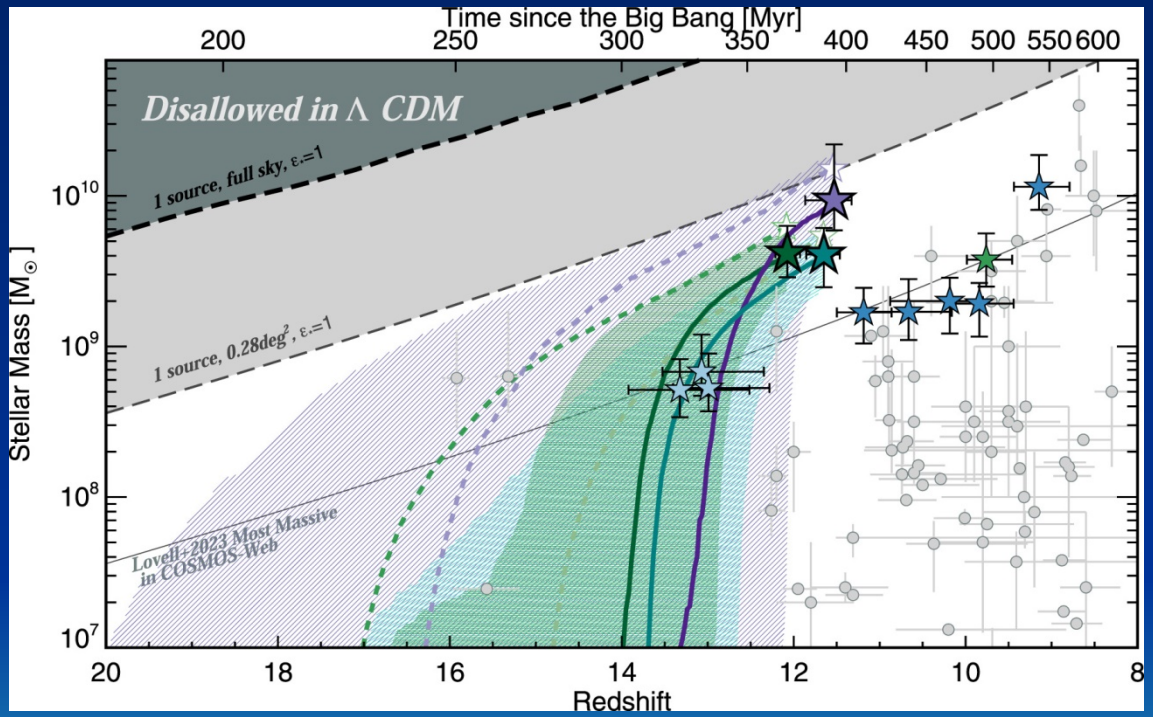

Варианты интерпретации

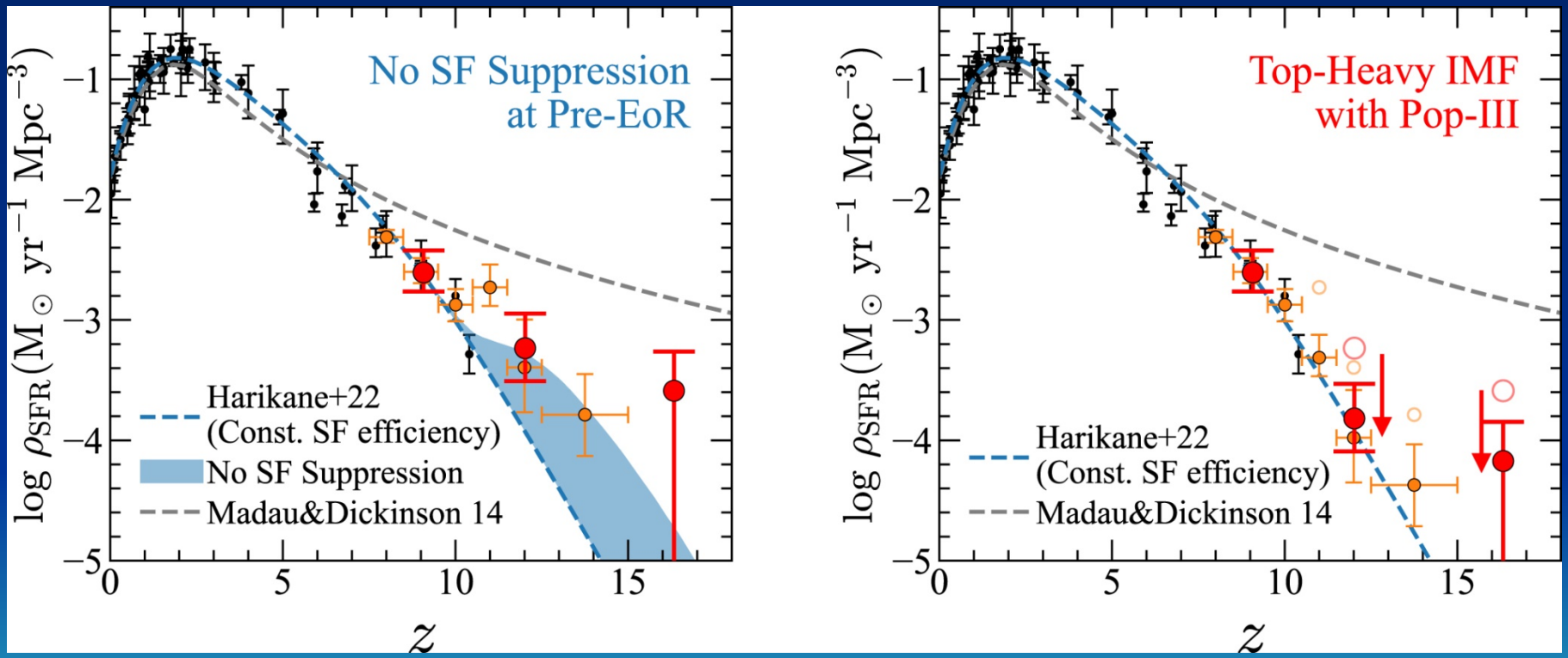

A quantitative definition of starbursts

Definition of a starburst: exceptional event, i.e. b > 2-3

b=SFR/<SFR>= birthrate parameter

Good proxy = specific SFR (SSFR) assuming same age:

sSFR= SFR/M* = SFR/<SFR> x 1/age

SFR/M* ~ 0.06 Gyr^{-1} (MW) → $\tau \approx 20$ Gyr time to build M_*

x 10 = 0.5 Gyr^{-1} (M82) → $\tau \approx 2$ Gyr

x 200 = 10 Gyr^{-1} (Arp220) → $\tau \approx 0.1$ Gyr

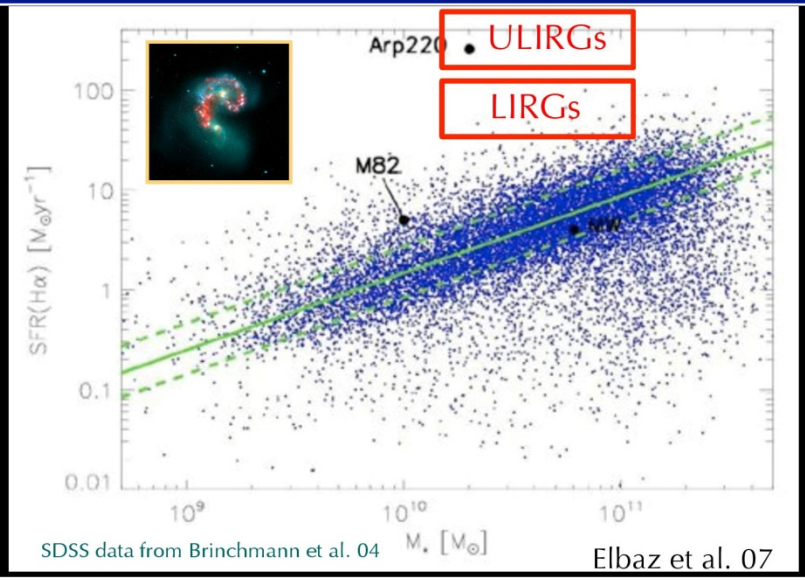

Главная последовательность на z=4-5

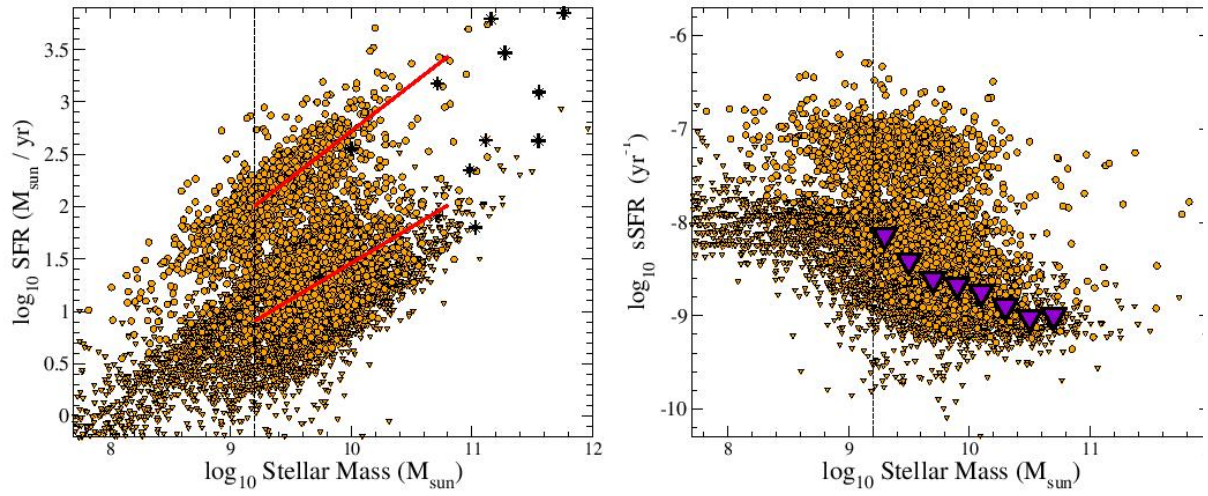

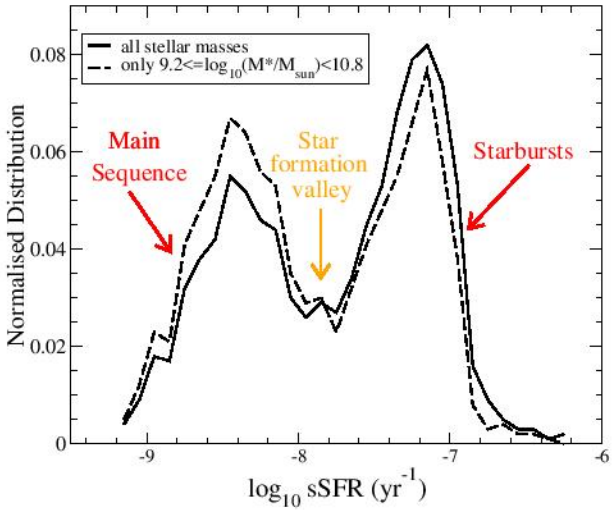

Figure 3. Normalised sSFR distribution of "Hα excess" galaxies at $3.9 \leq z \leq 4.9$. The main sequence and starburst galaxies are clearly separated at these redshifts. Here we denominate *'star formation valley'* to the region empirically determined to be at $-8.05 \leq \log_{10}(\mathrm{sSFR}) \leq -7.60$. This is analogue to the 'green valley' between the main sequence and passive regime, which is observed at lower redshifts.

Переходим к исследованию истории SF за последние 100 Myr

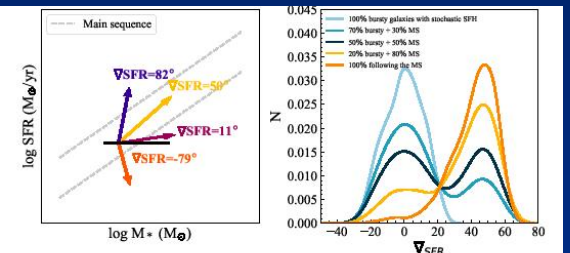

Fig. 7: Left panel: Schematic example of the definition of ∇SFR. The gradient corresponding to each arrow is indicated with the same color and show the path that galaxies followed recently. The point of the arrow indicate the position of the galaxy when observed. The black line is the reference from which the angle of the gradient is computed. The grey dashed lines mark the position of the MS with its the dispersion. Right panel: Mock distributions of ∇SFR obtained from simple modelling.

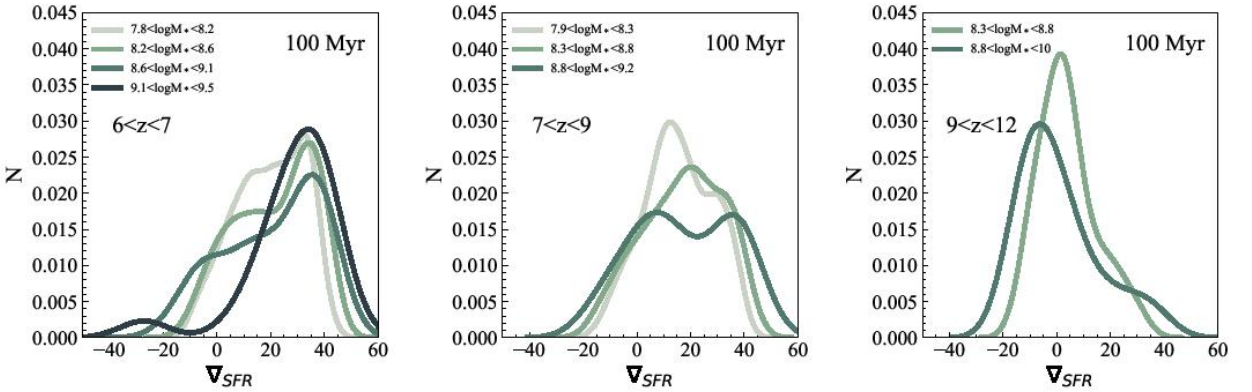

Fig. 8: Distribution of ∇SFR computed over 100 Myr in the three redshift bins. The different colors indicate different stellar mass bins.

Вспышечность слева, ламинарность справа

z>8: даже в массивных галактиках звездообразование идет вспышками

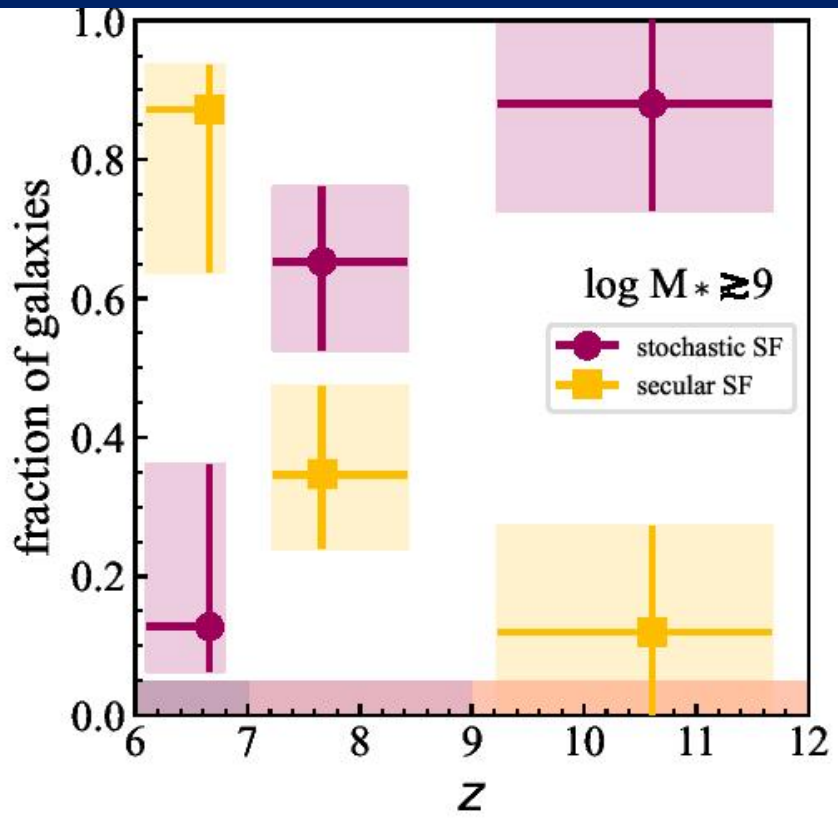

Fig. 9: Fraction of galaxies in the secular SFH gradient distribution (peak around 40°, yellow squares) and in the stochastic SFH distribution (peak around 0°, purple circles) as a function of redshift.

Ciesla+

Примеры индивидуальных историй звездообразования

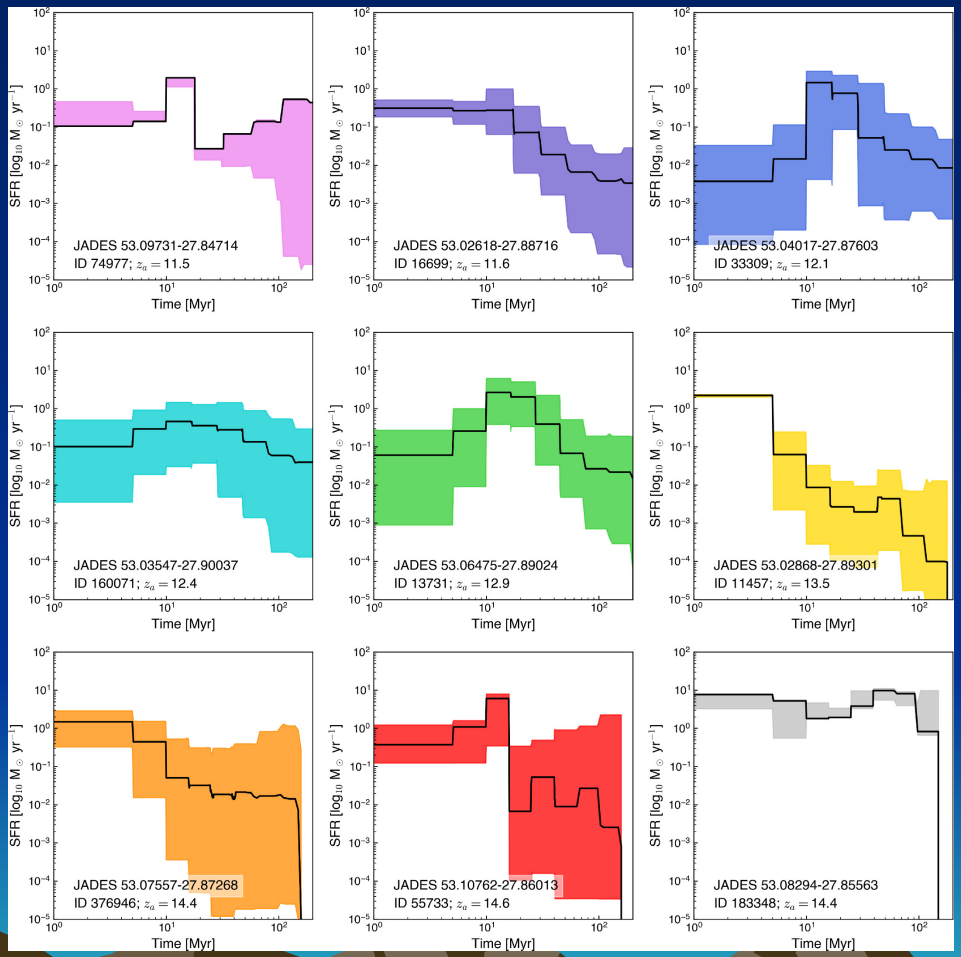

Robertson+(2024)

К чему все идет?

- JWST: слишком много массивных галактик и/или слишком высокий уровень космического звездообразования на z>10!
- Меняется физика звездообразования? Вспышечный режим? «Отвязка» истории звездообразования от истории сборки темного гало?